

Passive Line-of-Sight Stabilization for an Infrared Sensor

R. L. LUCKE

*Advanced Concepts Branch
Optical Sciences Division*

June 28, 1984



NAVAL RESEARCH LABORATORY
Washington, D.C.

Approved for public release; distribution unlimited

SECURITY CLASSIFICATION OF THIS PAGE

REPORT DOCUMENTATION PAGE				
1a REPORT SECURITY CLASSIFICATION UNCLASSIFIED		1b RESTRICTIVE MARKINGS		
2a SECURITY CLASSIFICATION AUTHORITY		3. DISTRIBUTION/AVAILABILITY OF REPORT Approved for public release; distribution unlimited.		
2b DECLASSIFICATION/DOWNGRADING SCHEDULE				
4. PERFORMING ORGANIZATION REPORT NUMBER(S) NRL Report 8828		5. MONITORING ORGANIZATION REPORT NUMBER(S)		
6a. NAME OF PERFORMING ORGANIZATION Naval Research Laboratory	6b. OFFICE SYMBOL (If applicable) Code 6520	7a. NAME OF MONITORING ORGANIZATION		
6c ADDRESS (City, State and ZIP Code) Washington, DC 20375		7b. ADDRESS (City, State and ZIP Code)		
8a. NAME OF FUNDING/SPONSORING ORGANIZATION Naval Air Systems Command	8b. OFFICE SYMBOL (If applicable) AIR 340J	9. PROCUREMENT INSTRUMENT IDENTIFICATION NUMBER		
8c ADDRESS (City, State and ZIP Code) Washington, DC 20361		10. SOURCE OF FUNDING NOS.		
11 TITLE (Include Security Classification) (See Page ii)		PROGRAM ELEMENT NO. 62712N	PROJECT NO. WF12-152-000	WORK UNIT NO. EX380-280
12. PERSONAL AUTHOR(S) Lucke, Robert L.				
13a. TYPE OF REPORT Final	13b. TIME COVERED FROM Sept. 82 TO Aug. 83	14. DATE OF REPORT (Yr., Mo., Day) 1984 June 28	15. PAGE COUNT 16	
16. SUPPLEMENTARY NOTATION				
17. COSATI CODES		18. SUBJECT TERMS (Continue on reverse if necessary and identify by block number)		
FIELD	GROUP	SUB. GR.	Stabilization Line-of-sight	
19 ABSTRACT (Continue on reverse if necessary and identify by block number)				
The use of passive gyroscopic stabilization in the vibrational environment of a P-3 aircraft is described theoretically. The conclusion is reached that even a fairly heavy instrument (30 kg) can have its line of sight stabilized to a precision of 100 μ rad or better.				
20 DISTRIBUTION/AVAILABILITY OF ABSTRACT UNCLASSIFIED/UNLIMITED <input checked="" type="checkbox"/> SAME AS RPT <input type="checkbox"/> DTIC USERS <input type="checkbox"/>		21 ABSTRACT SECURITY CLASSIFICATION UNCLASSIFIED		
22a NAME OF RESPONSIBLE INDIVIDUAL Robert L. Lucke		22b TELEPHONE NUMBER (Include Area Code) (202) 767-3045	22c OFFICE SYMBOL Code 6520	

DD FORM 1473, 83 APR

EDITION OF 1 JAN 73 IS OBSOLETE

SECURITY CLASSIFICATION OF THIS PAGE

11. TITLE (*Include Security Classification*) (Continued)

Passive Line-of-Sight Stabilization for an Infrared Sensor

CONTENTS

INTRODUCTION	1
EQUATIONS OF MOTION FOR A SPINNING ROTOR	2
EQUATIONS OF MOTION FOR A GIMBALED ROTOR	3
APPLICATION OF EQUATIONS OF MOTION TO A REAL SYSTEM	4
General Form of Driving Term and Resonance	4
Effect of Static and Dynamic Imbalance	7
Effect of Rotational Vibrations	8
CONCLUSIONS	10

PASSIVE LINE-OF-SIGHT STABILIZATION FOR AN INFRARED SENSOR

INTRODUCTION

A need exists for background data taken under realistic conditions to support the development of infrared (IR) surveillance systems for military applications. We propose to address this problem by mounting an existing IR scanner in the cabin of a Naval Research Laboratory (NRL) P-3 patrol plane. It is positioned to view the outside world through one of the P-3's forward observation windows (the plastic window material will be replaced by a pane of zinc selenide). This location permits the camera to be manually operated, which eliminates the need for a complicated and expensive remote control system.

As with any camera mounted on a moving platform, the instrument must be stabilized against the P-3's vibration environment. The sensor's 31.8 kg (70 lb) weight and 330 microradian (μrad) pixel size require the stabilization system to hold a heavy package on a fixed line of sight to an accuracy of 100 μrad so that no significant resolution degradation occurs. Problems of this kind are usually handled with an active stabilization system: gyroscopes attached to the instrument sense changes in direction and activate feedback loops, and torque motors keep the pointing direction constant. Such a system has the advantage of being fully automatic, with no operator required. However, it is very expensive, especially for three-axis stabilization to an accuracy of 100 μrad . The main reason for this is that errors introduced by the feedback loop and torque motors (especially the latter) require tighter tolerances for the mechanical system (particularly bearings) which can be met only by expensive, high-precision machining.

An alternate approach is to use passive stabilization, based on the principle that a gyroscope will resist rotation about an axis by precessing about a perpendicular axis. This principle is familiar from toy gyroscopes which, when supported at only one end, resist the force of gravity trying to rotate them around a horizontal axis by precessing around the vertical axis. This principle is applied to the sensor stabilization problem by attaching a gyroscope, gimballed about one axis, to the sensor, so that it is forced to move with the sensor in one direction, but is free to precess about its gimbal in a perpendicular direction (see Fig. 1). To quantify this principle, we first develop the equations of motion of a freely spinning rotor, then couple the rotor to a sensor package. The theory of gyroscopes has been exhaustively studied for hundreds of years, so no new physics need be developed; the discussion given here is tailored to our particular problem. The small angle approximation will be made in the equations of motion where appropriate: 0.1 mrad pointing stability will be lost long before the small angle approximation is violated. This permits a simple derivation of the root-mean-square response angle of the IR camera to a given sinusoidal input disturbance. This response can then be evaluated for the translational and rotational vibration environment of a P-3. We find that, for reasonable values of system mass and gyroscope rotor angular momentum, the stabilization system can easily counter the direct effects of vibrations. This leaves only mounting system flexure and bearing imprecision as the dominant disturbers of steady pointing.

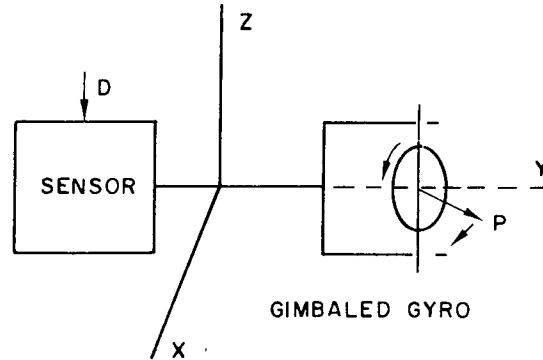


Fig. 1 - Schematic representation of gimbaled gyroscope attached to sensor. A disturbing force D in the $Y-Z$ plane results in precession P in the $X-Y$ plane.

EQUATIONS OF MOTION FOR A SPINNING ROTOR

The orientation of the angular momentum vector of the rotor is specified by the polar angles θ and ϕ ; ψ is the rotor's rotation angle: $\dot{\psi}$ = angular speed (see Fig. 2). The Lagrangian (which is just the kinetic energy in this case) for a spinning rotor¹ is

$$L = \frac{I_1}{2}(\dot{\theta}^2 + \dot{\phi}^2 \sin^2 \theta) + \frac{I_3}{2}(\dot{\psi} + \dot{\phi} \cos \theta)^2,$$

where I_3 is the moment of inertia about spin axis and $I_1 (= I_2)$ is the moment of inertia about the two perpendicular axes. This leads to the equation of motion for θ :

$$\frac{d}{dt} \left(\frac{\partial L}{\partial \dot{\theta}} \right) - \frac{\partial L}{\partial \theta} = I_1 \ddot{\theta} + (I_3 - I_1) \dot{\phi}^2 \sin \theta \cos \theta + I_3 \dot{\psi} \dot{\phi} \sin \theta = N_\theta = \text{external torque.}$$

Similarly, for ϕ and ψ :

$$\frac{d}{dt} \left[I_1 \dot{\phi} \sin^2 \theta + I_3 (\dot{\psi} + \dot{\phi} \cos \theta) \cos \theta \right] = N_\phi$$

$$\frac{d}{dt} \left[I_3 (\dot{\psi} + \dot{\phi} \cos \theta) \right] = N_\psi$$

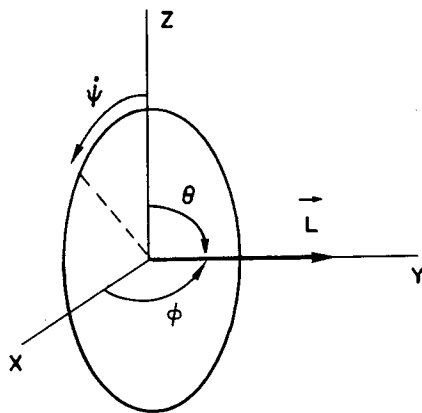


Fig. 2 - The direction of the rotor's angular momentum, L , is specified by the polar angles θ , ϕ . $\dot{\psi}$ is the rotor's angular speed.

¹H. Goldstein, *Classical Mechanics*, Addison Wesley Publishing Co., Inc., Reading, Massachusetts, 1965.

The rotor spins on nearly frictionless bearings, so $N_\psi \approx 0$, and is gimballed so it can turn freely about the vertical axis, so $N_\phi \approx 0$. Since we are interested in the stability of the gyroscope, we need to solve the equations of motion only for small angular displacements around an initial position. We therefore choose an initial position of $\theta = \pi/2$; this means $\sin \theta = 1$, $\cos \theta = 0$, and θ, ϕ, ψ are now independent angles, as a brief inspection of the Lagrangian shows. We therefore introduce the small-angle variable η :

$$\eta = \theta - \frac{\pi}{2}, \quad \sin \theta \approx 1 + 0(\eta^2), \quad \cos \theta \approx -\eta + 0(\eta^3).$$

The equations of motion are

$$I_1 \ddot{\eta} + (I_3 - I_1) \dot{\phi}^2 (-\eta) + I_3 \dot{\psi} \dot{\phi} = N_\theta$$

and

$$\frac{d}{dt} \left[I_1 \dot{\phi} + I_3 (\dot{\psi} + \dot{\phi}(-\eta)) (-\eta) \right] = 0$$

or, to first order in η , for the ϕ equation we have, without loss of generality

$$I_1 \dot{\phi} + I_3 \dot{\psi} (-\eta) = 0.$$

Note that $I_3 \dot{\psi} = L$ is the angular momentum of spinning rotor, so

$$\dot{\phi} = \frac{L}{I_1} \eta,$$

which, when substituted into the η equation gives, to 1st order in η :

$$I_1 \ddot{\eta} + L \cdot \frac{L}{I_1} \eta = N_\theta$$

or

$$\ddot{\eta} + \frac{L^2}{I_1^2} \eta = \frac{N_\theta}{I_1}.$$

As we expected from the small angle approximation, η undergoes simple harmonic motion with natural frequency $\omega_0 = L/I_1$, which is just the familiar nutation frequency found in gyroscope theory. Once η is found by solving this equation, ϕ , and therefore also $\dot{\phi}$, can be found immediately.

EQUATIONS OF MOTION FOR A GIMBALED ROTOR

We must now put the rotor in bearings in a housing and mount the housing (gimballed on one axis) on the package to be stabilized (this is shown schematically in Fig. 1). In the $\theta (= \eta + \pi/2)$ direction, the gyro and the package must move together, so the small-angle equation of motion is

$$I_T \ddot{\eta} + L \dot{\phi} = N_{\text{external}}, \quad (1)$$

as before, with I_1 replaced by the moment of inertia of the whole system computed about the stabilization axis. If the system is forced to move in the η direction, the gyro will, while it is resisting this motion, precess in the ϕ direction. Due to the gimbal bearings, this precession motion is *not* coupled to the package (as the θ motion was), so the ϕ equation of motion is the same as before:

$$I_G \dot{\phi} + L (-\eta) = 0 \Rightarrow \dot{\phi} = \frac{L}{I_G} \eta \quad (2)$$

once again, where I_G is the moment of inertia of the whole gyro (rotor and housing) computed about the gimbal axis.

For the case of a constant driving torque (DC input), we have, from Eq. (1), since $\ddot{y} \approx 0$,

$$\dot{\phi} = \frac{N}{L}.$$

Stabilization will remain good as long as $\phi \leq 1$ radian (larger ϕ means that the gyroscope has precessed until it is nearly parallel to the stabilization axis and can no longer stabilize). Now

$$\phi \approx \frac{N}{L}t,$$

so, if $L = 40 \text{ kg m}^2/\text{s}$ (which we expect), a DC torque of $1 \text{ N} \cdot \text{m}$ can be tolerated for about 40 s. In general, we can say that any constant torque, applied for a time τ such that $N\tau \leq 40$, will not exceed the capabilities of the stabilization system. This is important because the electrical cables and gas line (for the cryostat) attached to the sensor exert an approximately constant torque. This "attaching torque" can be minimized with good design, but should still be expected to precess the gyro through a large angle over time, a condition that will require operation intervention.

Combining Eqs. (1) and (2), the final equation of motion is now

$$\ddot{\eta} + \frac{L^2}{I_T I_G} \eta = \frac{N_\theta}{I_T}. \quad (3)$$

APPLICATION OF EQUATIONS OF MOTION TO A REAL SYSTEM

General Form of Driving Term and Resonance

The driving term on the right-hand side of Eq. (3) represents input to the stabilization system from translational and rotational vibrations of the aircraft. Coupling of rotational vibrations through the bearings on which the system gimbals are supported is negligible, as will be shown later. Coupling of rotational vibrations through viscous dampers mounted on the gimbal shafts is given by

$$\left(\frac{N}{I} \right)_{\text{damping}} = \gamma(\dot{\beta} - \dot{\eta})$$

where the angle β describes the angular motion of the airplane, so $\dot{\beta}$ and $\ddot{\beta}$ are the vibrational angular velocity and acceleration, respectively. The damping depends only on the difference between $\dot{\beta}$ and $\dot{\eta}$; if these two angular velocities are the same, the viscous dampers have no effect. Since the airplane's vibrations will be given as a Fourier spectrum $\beta = \beta_0 e^{i\omega t}$, we can write $\dot{\beta} = (1/i\omega)\ddot{\beta}$. With this part of the driving term separated out, the equation of motion becomes

$$\ddot{\eta} + \gamma\dot{\eta} + \frac{L^2}{I_T I_G} \eta = \frac{N}{I} e^{i\omega t} + \gamma \frac{\ddot{\beta}}{i\omega} e^{i\omega t}. \quad (4)$$

N/I now represents that part of the driving term which couples translational aircraft vibrations into rotational moments of the package—this will be calculated shortly. Writing the natural frequency of the system as $\omega_0 = (L^2/I_T I_G)^{1/2}$, we now have the generic equation for a damped harmonic oscillator driven by a sinusoidal input:

$$\ddot{\eta} + \gamma\dot{\eta} + \omega_0^2 \eta = D e^{i\omega t}.$$

The solution to this equation is

$$\eta = \frac{D}{\omega_0^2 - \omega^2 + i\omega\gamma} e^{i\omega t}.$$

Ordinarily, we are interested in the magnitude of η (not its phase) for a given drive term D . Hence we write

$$\left| \frac{\eta}{D} \right| = \frac{1}{\omega_0^2} \left\{ \frac{1}{\left[1 - \left(\frac{\omega}{\omega_0} \right)^2 \right]^2 + \left(\frac{\omega}{\omega_0} \right)^2 \left(\frac{\gamma}{\omega_0} \right)^2} \right\}^{1/2} \equiv \frac{1}{\omega_0^2} R.$$

Quantity R , the response normalized to unity at $\omega = 0$, is plotted in Fig. 3 for the case $\omega_0 = 2\pi \cdot 10 \text{ Hz} = 63 \text{ rad/s}$, $\gamma = 1 \text{ s}^{-1}$ (critical damping is $\gamma_c = 2\omega_0 = 126 \text{ s}^{-1}$, so the damping assumed here is quite small: $\gamma \lesssim 0.01 \gamma_c$).

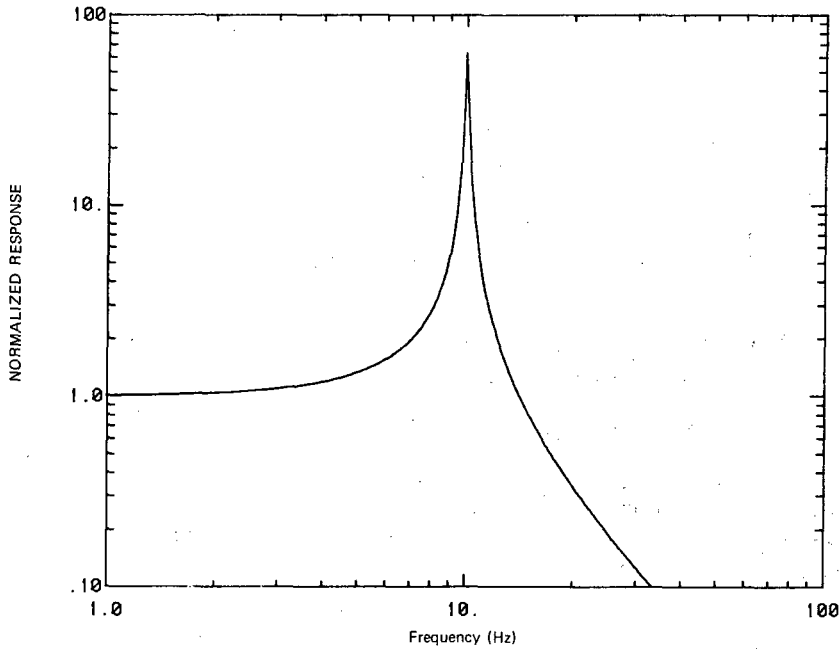


Fig. 3 — Normalized response of passive gyroscopic stabilizer with resonant frequency $F_n = 10 \text{ Hz}$. For total response multiply by $(2\pi F_n)^{-2}$.

As we shall see, the driving term D will be obtained from the vibration spectrum of a P-3 and will be given on a per square root of bandwidth basis, so the root mean square driving acceleration over a bandwidth Δf is $(D^2 \Delta f)^{1/2}$, and the total over all frequencies is $\left(\int_0^\infty D^2 df \right)^{1/2}$. Therefore, the total rms response of the system is given by $\eta_{\text{rms}} = [\eta_T^2]^{1/2}$, where

$$\eta_T^2 = \int_0^\infty |\eta|^2 df = \int_0^\infty \frac{D^2}{(\omega_0^2 - \omega^2)^2 + \omega^2 \gamma^2} df.$$

We anticipate a sharp resonance, $\gamma \ll \omega_0$, so virtually the entire contribution to the integral comes from within a few γ of ω_0 , where the integrand is well approximated by

$$\frac{D^2}{(\omega_0^2 - \omega^2)^2 + \omega^2 \gamma^2} \approx \frac{D^2}{4\omega_0^2} \cdot \frac{1}{(\omega - \omega_0)^2 + \left(\frac{\gamma}{2} \right)^2},$$

and $D(\omega) \approx D(\omega_0)$ is a constant over the narrow bandwidth of resonance. Therefore, using

$$d\omega = 2\pi df,$$

$$\eta_r^2 \approx \frac{D^2}{8\pi\omega_0^2} \int_0^\infty \frac{d\omega}{(\omega - \omega_0)^2 + \left(\frac{\gamma}{2}\right)^2},$$

$$\approx \frac{D^2}{4\omega_0^2\gamma}.$$

Hence

$$\eta_{rms} = \frac{D(\omega_0)}{2\omega_0\sqrt{\gamma}}. \tag{5}$$

This analysis assumes $D(\omega)$ is reasonably constant over ω , and may not be valid for cases where $D(\omega) \gg D(\omega_0)$ for some ω . This occurs in the P-3 for propeller harmonics at 17, 34, 68, and 136 Hz, which superimpose a discrete line spectrum on the vibrational continuum. The contribution from these discrete lines will be calculated separately later, and found to be negligible. P-3 vibration data for the forward observer's station are shown in Table 1 (see also Fig. 4).

Table 1 — Typical P-3 Vibrations for the Forward Observer's Station (from Lockheed). Note that 1 g = 10 m/s².

	Low-Frequency Continuum	17 Hz	34 Hz	68 Hz
Vertical	0.003 g/√Hz	0.01 g	0.03 g	0.06 g
Longitudinal	0.001	0.002	0.002	0.01
Lateral	0.002	0.002	0.006	0.1
Roll	<0.1 rad/s ² √Hz	<0.1 rad/s ²	1 rad/s ²	10 rad/s ²
Pitch	<0.05	0.05	0.05	0.6
Yaw	0.013	0.02	0.02	0.35

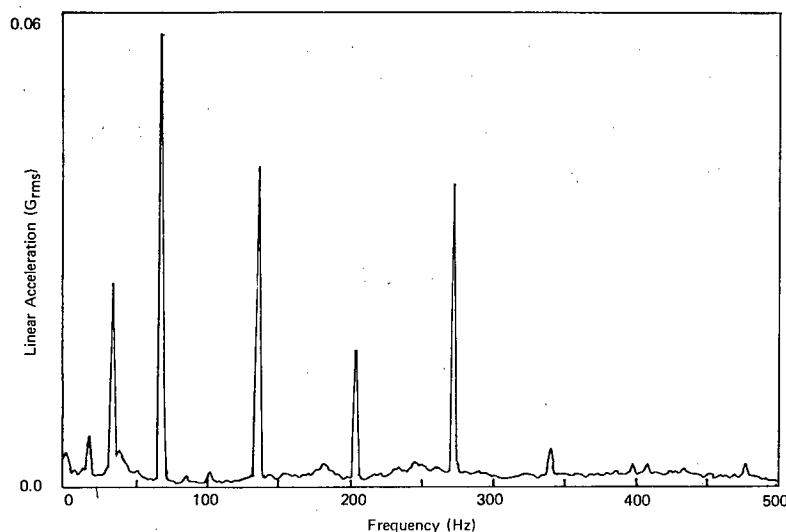


Fig. 4 — Typical vibration spectrum for P-3, forward observer's station

Effect of Static and Dynamic Imbalance

The dominant driving terms are due to imprecise static and dynamic balance of the package, resulting in aircraft linear accelerations coupling into rotational motions of the package. For static imbalance (referring to Fig. 5a): given a package with mass M and radius of gyration r (so $I = Mr^2$), out of balance by distance b , the torque resulting from a translational vibration of the support bearings given by $ae^{i\omega t}$ (a is the acceleration per $\sqrt{\text{Hz}}$) is

$$D = N/I = \frac{bMa}{Mr^2} = \frac{ba}{r^2}.$$

So, from Eq. (5),

$$\eta_{\text{rms}} = \frac{ba}{r^2} \cdot \frac{1}{2\omega_0\sqrt{\gamma}}.$$

Using

$$b = 0.001 \text{ m},$$

$$r = 0.3 \text{ m},$$

$$a = 0.1 \text{ m}/(\text{s}^2\sqrt{\text{Hz}}),$$

$$\omega_0 = 2\pi \cdot 10 \text{ Hz} = 63 \text{ rad/s}, \text{ and}$$

$$\gamma = (1 \text{ s})^{-1}$$

gives

$$\eta_{\text{rms}} = 10 \mu\text{rad}$$

which is well within the $100 \mu\text{rad}$ pointing stability required. Note that $a = 0.1$ is a generous estimate; it is a factor of 2 or more higher than actual P-3 vibration data.

A similar situation exists for dynamic imbalance (referring to Fig. 5b). For a differential linear acceleration between the support bearings of $ae^{i\omega t}$, the torque on the package is

$$\begin{aligned} N &= \left[cma \cdot \frac{l_2}{L} - cma \frac{l_1}{L} \right] e^{i\omega t} \\ &= cma \frac{l_2 - l_1}{L} e^{i\omega t} \approx cma e^{i\omega t}, \end{aligned}$$

so the driving term is

$$D = N/I = \frac{cma}{Mr^2} = \frac{ca}{r^2} \cdot \frac{m}{M}$$

Using

$$\frac{m}{M} = 0.02,$$

$$c = 0.5 \text{ m}, \text{ and}$$

$$a = 0.1 \text{ m}/(\text{s}^2\sqrt{\text{Hz}})$$

gives

$$\eta = 80 \mu\text{rad}$$

which is as much as can be tolerated. This shows that achieving $c \cdot (m/M) < 0.01$ m is desirable for dynamic balance, but we should again note that the value of 0.1 for a is too high, especially for the differential acceleration of the bearings.

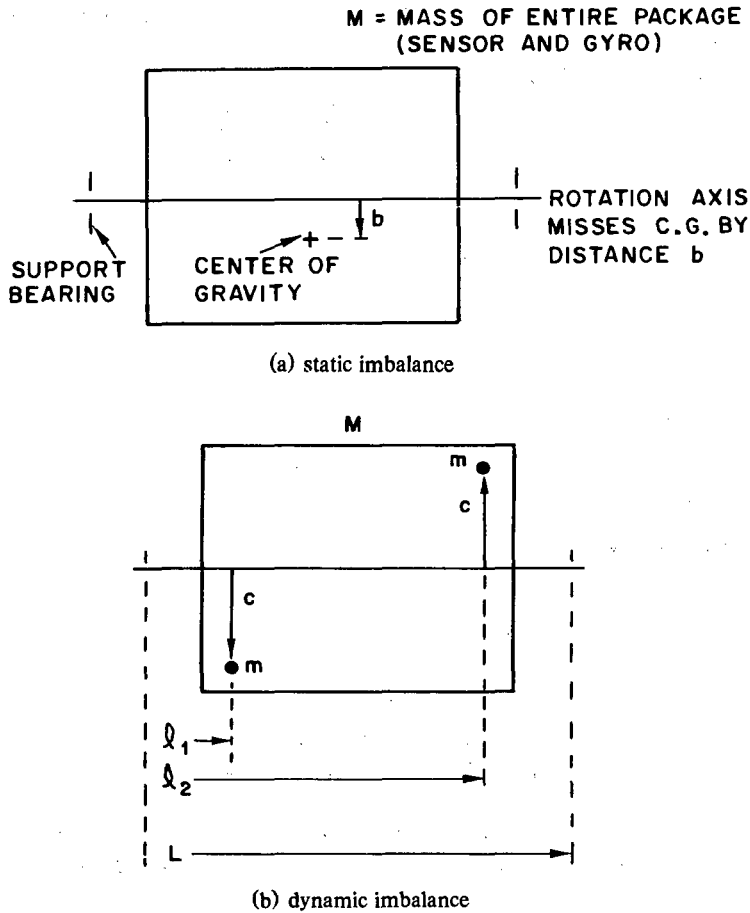


Fig. 5 — Geometry of (a) static and (b) dynamic imbalance. In (a), rotational motion of the package is induced by a translational acceleration of the support bearings perpendicular to the page, while in (b) a difference in the acceleration of the two bearings is required.

Effect of Rotational Vibrations

Rotational vibrations of the airplane are coupled to the package through the bearings on which it is mounted. According to bearing manufacturers (e.g. Fafnir Corporation), the torque transmitted through a bearing is nearly independent of load and angular velocity (unless they are very high), and can be expressed by

$$N = N_0 \text{Sgn} (\dot{\beta} - \dot{\eta})$$

where N_0 (\sim a few hundredths of a $\text{nt} \cdot \text{m}$) is a property of the bearing, and Sgn , the sign function, is ± 1 depending on the sign of its argument. If good stabilization is assumed, i.e., $\dot{\eta} \ll \dot{\beta}$, then $\dot{\eta}$ can be neglected and all we need to know about the above expression is how long the torque will have the same sign. An order of magnitude estimate of this time is

$$\tau \sim \dot{\beta}_{\text{rms}} / \ddot{\beta}_{\text{rms}}$$

i.e., the rms value of $\dot{\beta}$ divided by the rms value of its rate of change. Since

$$\ddot{\beta}_{rms} = \left[\int \ddot{\beta}^2 df \right]^{1/2}$$

and, from $\dot{\beta} = \frac{1}{i\omega} \ddot{\beta}$,

$$\dot{\beta}_{rms} = \left[\int \frac{1}{\omega^2} \ddot{\beta}^2 df \right]^{1/2}$$

we can find τ , once the angular vibration spectrum of the aircraft is known.

For a P-3, the continuum spectrum of $\ddot{\beta}$ is reasonably constant over the frequency range of interest, so it factors out of the integrals; τ can be easily estimated to be ≤ 0.1 s, using the low-frequency cutoff $f_c = 0.1$ Hz discussed below. Combining this with the low transmitted torque of the bearing, $N_0 \approx 0.01$ nt · m, shows that, since $N_0 t \sim 10^{-2} \ll 40$, this torque, caused by rotational vibration of the airplane, represents a completely negligible disturbance to the stabilization system.

For a given component of the P-3's discrete vibration spectrum, $\dot{\beta} = \beta_0 e^{i\omega t}$ and an adequate approximation to the driving torque can be obtained by noting that $\text{Sgn}(\dot{\beta}) \approx \text{Re}(e^{i\omega t})$, so that the driving term becomes

$$D e^{i\omega t} = \frac{N_0}{I} e^{i\omega t}.$$

The response to this drive is therefore

$$\eta = \frac{D}{\omega_0^2 - \omega^2 + i\omega\gamma} \approx \frac{N_0/I}{\omega_0^2 - \omega^2}$$

unless $\omega \approx \omega_0$. The first discrete frequency in a P-3 is $\omega = 2\pi \cdot 17$ Hz = 107 rad/s. As long as ω_0 is kept somewhat smaller than this, say $\omega_0 \approx 2\pi \cdot 10$ Hz = 63 rad/s. Then, using $N_0 \leq 0.01$ nt · m, $I \approx 10$ kgm², we find

$$\eta < 1 \mu\text{rad}.$$

The other and more important coupling of aircraft rotational vibrations to the package is through the rotational dampers used to limit the system response to resonance. Equation (5) suggests that γ should be large (heavy damping) to hold down the amplitude of the resonant peak, but Eq. (4) shows that a large γ increases the rotational vibration driving term, which is especially to be feared at low frequencies. A balance must be found. Setting $D(\omega_0) = \gamma\ddot{\beta}/\omega_0$, we find from Eq. (5) that the resonant response to continuum angular vibrations is,

$$\eta = \frac{\gamma\ddot{\beta}}{2\omega_0^2\sqrt{\gamma}} = \frac{\sqrt{\gamma}\ddot{\beta}}{2\omega_0^2}.$$

Using $\ddot{\beta} \leq 0.1$ rad/s² from P-3 vibration data and $\omega_0 \approx 60$ rad/s, $\gamma \approx 1$ s⁻¹ gives

$$\eta \approx 15 \mu\text{rad}.$$

The low-frequency response is

$$\eta = \left[\int_{f_c}^{f_{0/2}} \frac{(\gamma\ddot{\beta}/\omega)^2}{(\omega_0^2 - \omega^2)^2 + \omega^2\gamma^2} df \right]^{1/2}$$

where f_c is a low-frequency cutoff below which the continuum vibration spectrum does not extend. A conservative choice is $f_c = 0.1$ Hz. This choice is motivated by the fact that a sinusoidal angular acceleration of $\ddot{\beta} = 0.1$ rad/s² would require an angular motion of $\beta = \ddot{\beta}/\omega_c^2 \approx 0.3$ rad $\approx 15^\circ$, which does not happen on a P-3. Thus

$$\eta \leq \frac{\gamma\ddot{\beta}}{\omega_0^2} \left(\int_{f_c}^{f_{0/2}} \frac{1}{\omega^2} df \right)^{1/2} \approx \frac{\gamma\ddot{\beta}}{2\pi\omega_0^2\sqrt{f_c}} \approx 15 \mu\text{rad},$$

which shows that $\gamma \approx 1 \text{ s}^{-1}$ is a reasonable compromise. (Actually, γ will probably be a few times bigger than the 1% of critical assumed here, but f_c will be larger than 0.1 Hz in compensation.)

The vibration environment in the P-3 is composed of a continuum part, which is fairly constant over the range from 0 to 500 Hz, plus a discrete spectrum of propeller harmonics, of which the dominant components are at 17, 34, 68, and 136 Hz. At the forward observer's station (depending on how the propellers are synchronized) vibrations at these frequencies may exceed the continuum by a factor of 10 at 17 and 34 Hz, and as much as 100 at 68 and 136 Hz. A typical example of this vibration spectrum is shown in Fig. 4.

The stabilization system will be shock mounted in the P-3. Therefore, the vibration spectrum input to the stabilization system will be the P-3 vibration spectrum multiplied by the transmissibility of the shock mounts, which also (obviously) function as vibration isolators. The transmissibility of the shock mount system is given in Fig. 6, which shows that the discrete frequencies are suppressed by factors comparable to their enhancement above the continuum and hence are unimportant. This is done at the price of multiplying a section of the low-frequency continuum by the resonance peak of the mounting system—about a factor of 5. This presents a problem only if it coincides with the resonant frequency of the stabilization system. It also shows that the resonant frequency of the shock mounting system (about 5 Hz) must be kept reasonably separate from the resonant frequency of the stabilization system (about 10 Hz).

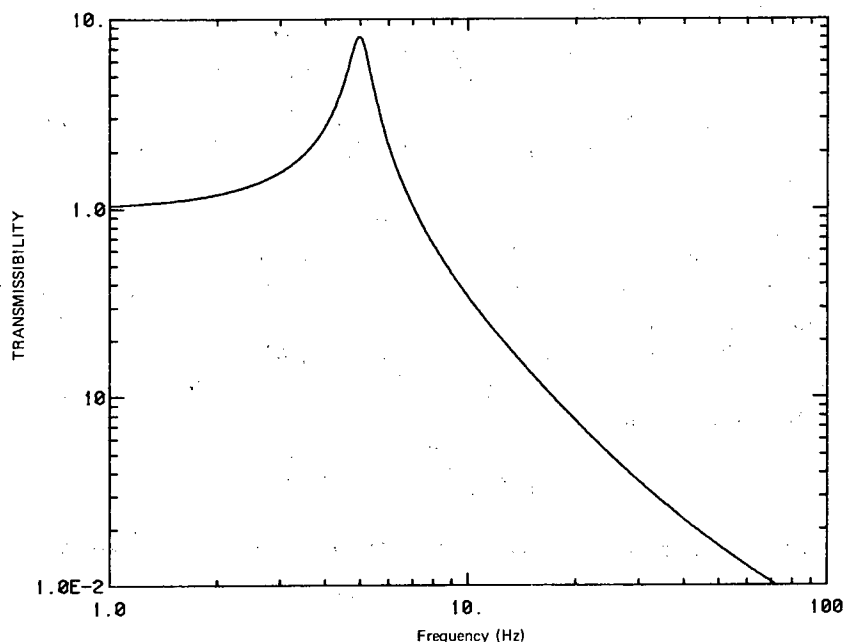


Fig. 6 — Transmissibility of typical shock mounting system, $F_n = 5 \text{ Hz}$

CONCLUSIONS

The foregoing analysis shows that with proper balance of the package and care taken in preparing the shock isolation system, the passive approach to stabilization can easily handle the vibrational environment of a P-3. The stabilization system itself does not introduce unacceptable errors. This leaves only the mechanical tolerances of the mounting system: if a shaft is mounted on two ball bearings 50.8 cm (20 in.) apart and each ball bearing has $25.4 \mu\text{m}$ (0.001 in.) of imprecision (this is typical

for standard bearings, higher precision bearings are available only on special order), the shaft could be expected to have an extreme wobble of $\pm 50 \mu\text{rad}$. Combined with a small amount of flexure in the shaft itself, this shows that the main constraints on pointing stability are mechanical in nature and can be solved by standard design techniques.